

Elasto-Plastic-Creep Constitutive Equation of an Al-Si-Cu High-Pressure Die Casting Alloy for Thermal Stress Analysis



YUICHI MOTOYAMA, HIDETOSHI SHIGA, TAKESHI SATO, HIROSHI KAMBE,
and MAKOTO YOSHIDA

Accurate simulation of residual stress and deformation is necessary to optimize the design and lifetime of casting components. Therefore, the recovery and strain-rate dependence of the stress-strain curve have been incorporated into empirical constitutive equations to improve the thermal stress analysis accuracy. Nevertheless, these equations present several difficulties related to the determination of material constants and their physical bases. This study suggested an empirical elasto-plastic-creep constitutive equation incorporating these phenomena. To determine the material parameters used in this constitutive equation, this study investigated tensile test methods to obtain stress-strain curves that most closely resemble those during or immediately after casting for the Al-Si-Cu high-pressure die-casting alloy JIS ADC 12 (A383.0), which exhibits natural aging. Results show that solution heat treatment with subsequent cooling to the test temperature should be applied to obtain stress-strain curves used for the thermal stress analysis of high-pressure die casting process of this alloy. The yield stresses obtained using the conventional heating method were 50-64 pct higher than those of the method described above. Therefore, the conventional method is expected to overestimate the overestimation of the predicted residual stress in die castings. Evaluation of the developed equation revealed that it can represent alloy recovery and strain-rate dependence.

DOI: 10.1007/s11661-016-3734-x

© The Minerals, Metals & Materials Society and ASM International 2016

I. INTRODUCTION

RESIDUAL stress and deformation in castings are crucially important issues not only for producing components having a highly precise shape but also for managing the life of casting components. Therefore, for the casting process, several researchers have tackled these problems using thermal stress analysis conducted *via* computer-aided engineering. The constitutive equation of the casting alloys strongly affects the predictive accuracy of residual stress and the deformation that occurs during casting. Therefore, accurate prediction demands selection of an appropriate constitutive equation and the use of mechanical properties of the casting alloy. Researchers have strived to measure the mechanical behaviors of casting alloys and to develop

constitutive equations for them from low to high temperature ranges. This study specifically examines the development of the constitutive equation of an Al-Si-Cu high-pressure die casting alloy [Japanese Industrial Standard (JIS) ADC12 (A383.0)]. The following sections respectively present discussion of earlier studies related to the mechanical properties of the Al-Si-Cu high-pressure die casting alloy and to constitutive equations for the casting process.

A. Mechanical Properties Required for the Constitutive Equation

Mechanical properties of Al-Si-Cu high-pressure die casting alloys have been measured from room temperature (RT) to the high temperature range. The obtained values have been used by several researchers for thermal stress analyses. Garza *et al.*^[1] conducted elevated temperature tensile tests to ascertain the mechanical properties of the high-pressure die casting alloy A380.0 for computer prediction of the residual stress and of the casting distortion. Makhlof *et al.*^[2] obtained stress-strain curves of various high-pressure die casting alloys from RT to 473 K (200 °C). However, their study did not measure stress-strain curves at temperatures higher than 473 K (200 °C). Therefore, their material property data are insufficient to conduct accurate thermal stress analyses of the casting. Dong *et al.*^[3] measured stress-strain curves of Al-Si-Cu aluminum high-pressure die casting alloy from 298 K to 773 K (25 °C to 500 °C)

YUICHI MOTOYAMA, Researcher, is with the Department of Modern Mechanical Engineering, Waseda University, 3-4-1 Ookubo, Shinjuku-ku, Tokyo, 169-0072, Japan (now Advanced Manufacturing Research Institute, National Institute of Advanced Industrial Science and Technology, 1-2-1, Namiki, Tsukuba, Ibaraki, 305-8564, Japan). Contact email: y.motoyama@aist.go.jp HIDETOSHI SHIGA and TAKESHI SATO, Engineers, and HIROSHI KAMBE, Expert Leader, are with the Powertrain Technology and Prototype Development Department, Nissan Motor Co. Ltd., 6-1, Daikokucho, Tsurumi-ku, Yokohama-shi, Kanagawa, 230-0053, Japan. MAKOTO YOSHIDA, Professor, is with the Kagami Memorial Research Institute for Material Science and Technology, Waseda University, 2-8-26, Nishiwaseda, Shinjuku-ku, Tokyo, 169-0051, Japan.

Manuscript submitted January 28, 2016.

Article published online August 25, 2016

using tensile tests to simulate the thermal stress of the die casting component. Actually, Al-Si-Cu high-pressure die casting alloys are known to exhibit aging behavior immediately after casting parts (herein, “as-cast” denotes the state during or immediately after casting), even at RT: natural aging (N.A.). However, earlier reports described tensile tests conducted simply by heating the specimen from RT to the testing temperature (heating test or H.T.), often with no note whatsoever of the aging state of the tensile test specimen. Therefore, the mechanical properties obtained from these earlier studies are expected to differ greatly from those of casting during cooling because the precipitation state in the tensile specimen probably changes during the period immediately after casting of the specimen to tensile testing. In that case, because of precipitation hardening, the obtained yield stresses are probably higher than those of the as-cast state. The use of these mechanical properties is expected to engender unreliable estimation of the residual stress and of the casting deformation.

To address this difficulty, Magnin *et al.*^[4] applied solution heat treatment (SHT) to specimens before cooling to each tensile testing temperature to obtain equivalent mechanical properties to those of the Al-4.5 pctCu alloy in the as-cast condition to the greatest extent possible (cooling-test or C.T.). By conducting SHT, dissolution of the existing precipitate is expected in tensile specimens before stretching. However, no report of the relevant literature describes a study of the different mechanical properties of C.T. and H.T. This comparison must be conducted to discuss more suitable mechanical properties for thermal stress analysis of precipitate-hardening-type aluminum alloys.

This study was conducted to assess the effects of C.T. on stress–strain curves of the N.A. ADC12 casting specimen. First, the effects of SHT were investigated by comparing the respective hardness of casting specimens of SHT, N.A., and the as-cast condition. In addition, the effect of the holding time at the SHT temperature on hardness was studied to ascertain the SHT condition for the C.T. The comparison revealed that the hardness of the N.A. specimen approximates that of the as-cast condition specimen by SHT. Finally, the stress–strain curves of the alloy were measured using C.T., for which the SHT condition was the same as that of the hardness test described above. These curves were compared with those obtained using conventional H.T. to assess the different results obtained using the two test methods.

B. Constitutive Equation for Thermal Stress Analysis of the Casting Process

The strain-rate dependence of the stress–strain curve (strain-rate dependence) and the recovery are well-known mechanical behaviors that occur at high temperatures in various alloys. Millar^[5] reported an equation that can represent these metallurgical phenomena accurately based on the internal variables theory. However, this equation requires numerous material constants and complex experiments to obtain these constants. Therefore, empirical elasto-plastic, elasto-viscoplastic, and

elasto-plastic-creep constitutive equations have been developed and used in several earlier studies.

The elasto-plastic constitutive equation, the classical constitutive equation, is often used for thermal stress analyses, especially for shape castings. Gustafsson *et al.*^[6] simulated the residual stress developed in a gray cast iron casting using the elasto-plastic model. Hofer *et al.*^[7] simulated the thermal stress of simple aluminum high-pressure die casting components. Dong *et al.*^[3] predicted cold cracking of the ADC12 component and proposed a method for predicting cold cracking. Motoyama *et al.*^[8] simulated the residual stress attributable to the temperature difference between thick and thin parts of the gray cast iron casting. They also investigated the residual stress attributable to the temperature difference in the cross section of the casting.^[9]

The following equations were often used in earlier studies.

$$\varepsilon_{ij} = \varepsilon_{ij}^e + \varepsilon_{ij}^p \quad [1]$$

$$\sigma_{ij} = D_{ijkl}(T)\varepsilon_{kl}^e \quad [2]$$

$$f(\sigma_{ij}, T) = \sqrt{3J_2} - \sigma_y(T) - K \quad [3]$$

$$K = K(\varepsilon_{eff}^p, T) \quad [4]$$

$$\dot{\varepsilon}_{ij}^p = \lambda \frac{\partial f}{\partial \sigma_{ij}} \quad [5]$$

Here, T stands for the temperature, σ_{ij} denotes the stress, ε_{ij}^e signifies the elastic strain, ε_{ij}^p represents the plastic strain, D_{ijkl} is the elastic coefficient tensor, J_2 is the second invariant of the deviatoric stress tensor, and $\sigma_y(T)$ represents the initial yield stress dependent on the temperature. In addition, ε_{eff}^p stands for the equivalent plastic strain, λ denotes the positive scalar, and K is the hardening parameter, which is a function of the temperature and equivalent plastic strain. However, the elasto-plastic constitutive equation presented above engenders several difficulties related to the thermal stress analysis of the castings. Generally, the elasto-plastic constitutive equation cannot represent the strain-rate dependence. In addition, as shown in [3] and [4], the equivalent plastic strain increment developed at each temperature accumulates in the same manner. Therefore, even the equivalent plastic strain developed at a high temperature range contributes to strain hardening at a low temperature in the same manner as that developed in the low temperature range. The recovery is not considered in the elasto-plastic constitutive equation. This behavior causes an unrealistic increase of the initial yield stress at the low temperature. Therefore, the use of an elasto-plastic constitutive equation is expected to engender overestimation of the residual stress in castings.

The elasto-viscoplastic constitutive equation treats the inelastic strain as one quantity: viscoplastic strain. The

following equation is an elasto-viscoplastic constitutive equation that has been used widely for thermal stress analysis of the shape castings.

$$\varepsilon_{ij} = \varepsilon_{ij}^e + \varepsilon_{ij}^{vp} \quad [6]$$

$$\sigma_{ij} = D_{ijkl}(T)\varepsilon_{kl}^e \quad [7]$$

$$\sigma_{\text{eff.}} = F(\varepsilon_{\text{eff.}}^{vp}, \dot{\varepsilon}_{\text{eff.}}^{vp}, T) \quad [8]$$

Here, $\sigma_{\text{eff.}}$ signifies the equivalent stress, $\varepsilon_{\text{eff.}}^{vp}$ denotes the equivalent viscoplastic strain, and $\dot{\varepsilon}_{\text{eff.}}^{vp}$ stands for the rate of the equivalent viscoplastic strain. The elasto-viscoplastic constitutive equation incorporates strain-rate dependence. Thorborg *et al.*^[10] predicted the residual stress of the cast iron casting using a time-dependent model and showed that their model predicted the measurement more accurately than the time-independent model. However, the elasto-viscoplastic constitutive equation is normally not able to incorporate consideration of the recovery for the same reason as the elasto-plastic constitutive equation. Therefore, the use of the elasto-viscoplasticity constitutive equation also presents the possibility of an unrealistic increase of the initial yield stress at low temperatures.

Several researchers have attempted to incorporate recovery into the equations described above in the thermal stress analysis, especially for the direct chill casting process. Ejær and Mo^[11] used the “cut-off temperature” above which the developed inelastic strain did not accumulate in the effective plastic strain, which indicated the degree of strain hardening. Dretzet *et al.*^[12] also used the cut-off temperature method for the elasto-viscoplastic constitutive equation to predict the residual stress in the aluminum billet. However, it is not reasonable that the inelastic strain developed below one temperature suddenly starts to accumulate. Alankar and Wells^[13] divided the inelastic strain developed at each temperature into “plastic strain” and “creep strain.” The former strain component was included in strain hardening. The latter strain component was not. The temperature dependence of the ratio of the creep strain was determined using the strain hardening exponent of each temperature. Their constitutive equation can represent the temperature dependence of the recovery behavior smoothly. However, the temperature dependence of the recovery behavior is not physically related to the strain hardening exponent at each temperature. This fact engenders a lack of a physical basis for representation of the recovery behavior in their model. Haafte *et al.*^[14] assessed the temperature dependence of the recovery behavior of wrought aluminum alloys experimentally. The following constitutive equation was suggested to represent its recovery behavior.

$$\sigma_H = \left(\sigma_0 + k\sqrt{\alpha(T)\varepsilon} \right) \cdot f(Z) \quad [9]$$

Therein σ_H represents the yield stress, k is a constant, ε stands for the effective plastic strain, and $\alpha(T)$

represents the recovery ratio ($0 \leq \alpha(T) \leq 1$) at temperature T . The effective plastic strain was multiplied directly by the recovery ratio. Function $f(Z)$ is defined as shown below.

$$f(Z) = \min \left(1, \arcsin h \left(\left(\frac{Z}{A} \right)^{mH} \right) \right) \quad [10]$$

In that equation, Z stands for the Zener–Hollomon parameter. A and mH are material constants. The simple multiplication of $\alpha(T)$ is useful for simulating the recovery behavior at a given temperature. However, the strain component of the recovery is not subtracted from the developed plastic strain according to $\alpha(T)$ in Eq. [9]. Therefore, the plastic strain developed at all temperature ranges eventually accumulates and causes the unrealistic increase of the initial yield stress at a low temperature range in their equation.

For this study, the inelastic strain developed at the steady-state flow stress region of the stress–strain curves at high temperatures was assumed not to contribute to strain hardening at low temperatures. This assumption is reasonable because the strain hardening and softening attributable to the dynamic recovery are balanced in the region. On this physical basis, the other aim of this study is to suggest an elasto-plastic-creep constitutive equation that can represent both the strain-rate dependence and recovery (Japan Patent Kokai 2015-132564).^[15] For our purposes, the suggested constitutive equation is developed for ADC12 (A383.0). The reproducibility of the stress–strain curves at each temperature and the recovery behavior are presented in the evaluation of this constitutive equation.

II. EXPERIMENTAL PROCEDURES

A. Hardness Test

The chemical compositions of the alloy used in the hardness tests are presented in Table I(a). Ingots of the alloy were melted at 1073 K (800 °C). Degassing of the molten alloy was conducted with 0.3 l/min and 4 minutes Ar gas bubbling immediately before pouring. The liquidus and solidus temperatures of the alloy were, respectively, 845 K and 763 K (572 °C and 490 °C). To cast the specimens, a hollow steel column mold was put on a steel chill plate without preheating. Then a K-type stainless steel probe (φ : 2.3 mm \times L: 200 mm) thermocouple was inserted into the cavity center. Molten aluminum alloy was poured into the cavity at 1023 K (750 °C). The specimens were quenched in the water when the temperature reached 723 K (450 °C). The specimen diameter and height were, respectively, 41 and 30 mm. Five column specimens were cast. From the column specimens, disk-shaped specimens were cut off from the chilled surface to 5 mm thickness using a fine cutter for use in the hardness tests. Immediately after quenching, one specimen was cut off and was used to ascertain the hardness in the as-cast condition with a Rockwell F scale hardness testing machine. This

Table I. Chemical composition of ADC12 for (a) hardness test and (b) tensile specimen

	Si	Cu	Mg	Zn	Fe	Mn	Ti	Ni	Al
(a) Mass Pct	10.800	2.160	0.210	0.830	0.790	0.220	0.040	0.070	bal.
(b) Mass Pct	10.850	1.680	0.280	0.748	0.757	0.243	0.060	0.058	bal.

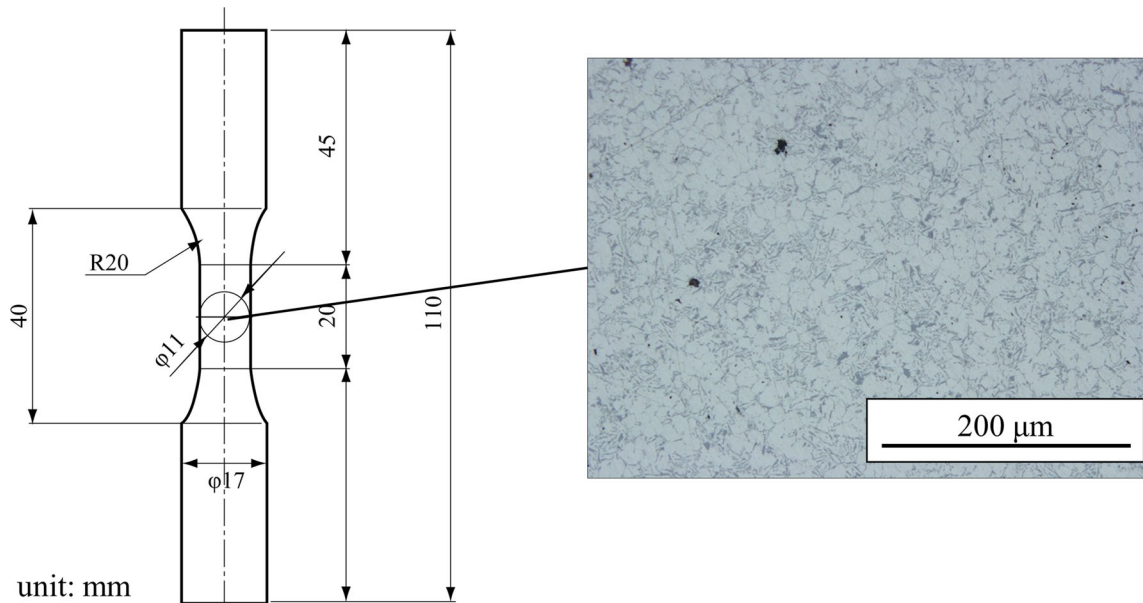


Fig. 1—Dimensions of PF die casting specimen and microstructure in the gage section.

hardness test was conducted immediately (within 1 hour) after producing the specimen. N.A. was not observed within 1 hour. The other four disk-shaped specimens were aged for 1 week at RT. The three N.A. specimens were heated in a furnace at 723 K (450 °C) for 1 hour, 2, or 3 hours to assess the effects of the heating time on hardness. These specimens were quenched in the water immediately after heating at that temperature. The last disk-shaped specimen of the N.A. specimens was used to measure hardness in the N.A. condition. All hardness tests were conducted at six points on the cross section surface of the disk specimens. The average of the measurements taken at the six points is presented as the hardness test results.

B. Young's Modulus

Young's modulus of the alloy was measured using the resonance method, a nondestructive method, at RT, 423 K, 473 K, 523 K, 573 K, 623 K, 673 K, and 723 K (150 °C, 200 °C, 250 °C, 300 °C, 350 °C, 400 °C, and 450 °C). The samples were cast in a copper mold and were machined for the specimens. The machined test specimen dimensions were 90 × 10 × 2 mm. The difference of the measured results was within 1 pct between the H.T. and C.T. method in preliminary measurements

at 473 K and 523 K (200 °C and 250 °C). This result seems reasonable because Young's modulus is a physical property: it is not sensitive to the metallographic structure. Therefore, the measurements were conducted using the H.T. method alone.

C. Tensile Test

1. Tensile specimen and testing machine

Figure 1 shows the tensile specimens that were produced using the pore-free (PF) high-pressure die casting process. The chemical composition of the alloy is presented in Table I(b). All tensile specimens were inspected using X-ray radiographic testing to check the shrinkage in the gage section. Visible shrinkage in the gage section was observed in no specimen. These specimens were aged at RT for 2 weeks before tensile tests. Subsequently, the tensile specimens were machined from as-cast dimensions, as presented in Figure 2. Tensile tests were conducted using the MTS810 Material Test System attached to a high-temperature extensometer (MTS 632.54F-14 Gage length = 12 mm) with which the tensile strain rate was controlled during loading. The temperature distribution was ±5 K in the gage section of the tensile specimen during testing.

2. Cooling test

For the cooling test, specimens were heated at a rate of 23 K/min from RT to 723 K (450 °C) and were solutionized for 1 hour to dissolve the precipitate in the specimens (Figure 3). This SHT condition was determined preliminarily based on results of the hardness test described later. Figures 4(a) and (b) respectively show the microstructures of the as-cast tensile specimen and a specimen after SHT at 723 K (450 °C) for 1 hour. From that comparison, no coarsening of the microstructure was observed. Changes of the mechanical properties are

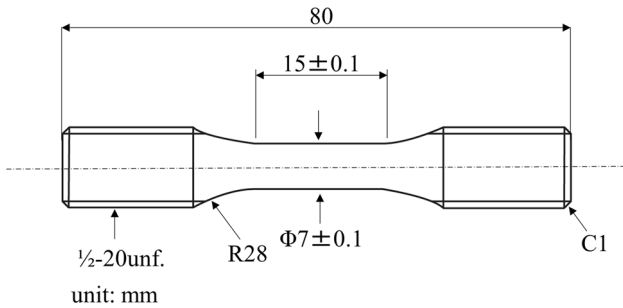


Fig. 2—Dimensions of tensile test specimens.

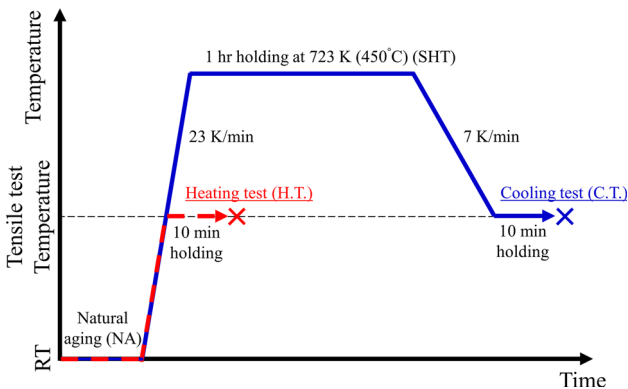


Fig. 3—Temperature histories in both heating and cooling tensile tests.

expected to result only from the precipitation state change in the specimen. It is probably favorable for the cooling rate after the SHT to be the same as that of the actual casting condition.^[16] However, the maximum cooling rate achieved in the testing machine we used was 7.5 K/min. That cooling rate was adopted for the cooling test. The tensile specimens were held for 10 minute at the testing temperatures before straining to homogenize the temperature distribution in the gage section. The testing temperatures were RT (only 0.001/s), 423 K, 473 K, 523 K, 573 K, 623 K, 673 K, and 723 K (150 °C, 200 °C, 250 °C, 300 °C, 350 °C, 400 °C, and 450 °C). The tensile strain rates were 0.001 and 0.0001/s. These strain rates were assessed by analyzing the cooling rates (thermal strain rates) of a typical aluminum high-pressure die cast automobile cylinder block.

3. Heating test

Conventional H.T. was also conducted to investigate the effects of natural aging on stress–strain curves. The tensile specimens were prepared using the same conditions and dimensions as those used for C.T. The tensile specimens were heated directly from RT to each testing temperature at 23 K/min and were held for 10 minutes before straining (Figure 3). The H.T. was conducted only at RT, 423 K, 473 K, and 523 K (150 °C, 200 °C, and 250 °C) at the strain rate of 0.001/s because the solo aim of this test was comparison with the results of C.T.

III. SUGGESTED ELASTO-PLASTIC-CREEP CONSTITUTIVE EQUATION

Stress σ is assumed to be caused solely by elastic strain ϵ_e . The rate form of the mechanical model in the uniaxial loading is the following.

$$\dot{\sigma}_{ij} = E_{ijkl} \dot{\epsilon}_{kl}^e \quad [11]$$

The equation below shows that the total strain is divisible into elastic, plastic, creep, and thermal strain.

$$\dot{\epsilon}_{ij} = \dot{\epsilon}_{ij}^e + \dot{\epsilon}_{ij}^p + \dot{\epsilon}_{ij}^c + \dot{\epsilon}_{ij}^t \quad [12]$$

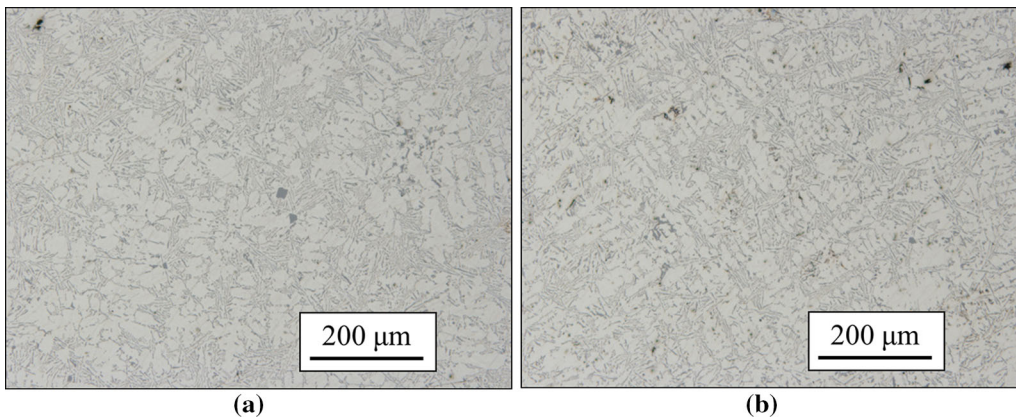


Fig. 4—Microstructure of ADC12 tensile specimen: (a) as-cast condition and (b) SHT at 723 K (450 °C) for 1 h.

Components of the plastic and creep strains of each temperature were determined as described hereinafter.

A. High Temperature Range

In this temperature range, the stress–inelastic strain curve has a large part of the steady flow stress (steady state) region following the small part of the strain hardening region. The steady-state stress has strain-rate sensitivity. The leftmost figure in Figure 5 presents a schematic illustration of this behavior. It was assumed for this study that the stress–inelastic strain curve was divided into a strain hardening region and a steady-state region. The steady-state region, which contributes dominantly to the amount of the inelastic strain at the high temperature range, can be represented using the steady-state creep equation (solid line in the rightmost figure in Figure 5). The plastic constitutive equation was inputted as a line to represent the initial strain hardening region (broken line in the middle figure in Figure 5). Consequently, the unrealistic accumulation of the plastic strain that contributes to excessive strain hardening can be avoided in the high temperature range.

For this study, the Norton law was used as the steady-state creep law.

$$\dot{\epsilon}_c = A\sigma^n \quad [13]$$

In this equation, A and n are material parameters. Actually, A and n -values are well known to be functions not only of temperature but also stress. However, the strain-rate range considered in this study was narrow: 0.001 to 0.0001/s. Therefore, in this study, A and n -values were assumed to be constant at one temperature and to be a function only of temperature.

In the plastic constitutive equation, the von Mises yield function, the isotropic hardening law, and the associated flow rule were adopted.

B. Middle and Low Temperature Range

With decreasing temperature, the stress–inelastic strain curves exhibit a gradual increase of strain hardening and a gradual decrease of the strain-rate dependence. To simulate this stress–inelastic strain behavior, the developed constitutive equation made the creep term ineffective by changing the value of creep parameter “ A ” to almost 0. As a result, the

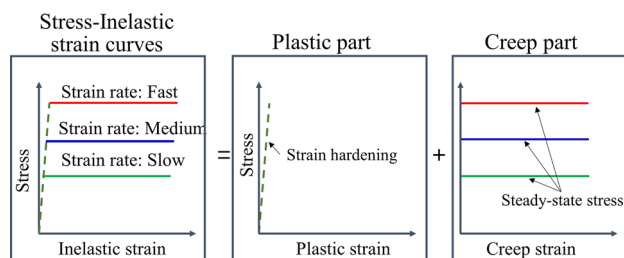


Fig. 5—Schematic illustration of dividing stress–strain curves in a high temperature range into plastic and creep part.

elasto-plastic-creep constitutive equation changes to an almost elasto-plastic constitutive equation. Therefore, it is unsuitable for this constitutive equation to show simultaneous expression of both strain-rate dependence and slight strain hardening of the stress–inelastic strain curve observed in the middle temperature range. At its temperature range, the stress–inelastic strain curves obtained at each tensile strain-rate were averaged. The averaged stress–inelastic strain curves were used for the stress–plastic strain relation in the almost elasto-plastic constitutive equation described above.

The following evaluation of the developed constitutive equation was conducted using the commercial finite element software Abaqus standard.

IV. EXPERIMENTAL RESULTS AND DISCUSSION

A. Hardness Test

Figure 6 presents results of the as-cast, N.A., and SHT hardness tests. Hardness of the as-cast condition increased by approximately 10 points (13 pct higher) after application of N.A. for 1 week. However, by executing SHT on the N.A. specimen, its hardness showed a 5 pct difference compared with the as-cast condition. These results indicate that the precipitation state would become close to that of the as-cast condition because of dissolution of the precipitation by SHT. The C.T. method is expected to obtain stress–strain curves approximating those of the as-cast condition. Figure 7 shows the effect of the SHT time on the hardness. This result demonstrates that 1 hour at 723 K (450 °C) is sufficient for dissolution of the precipitation in the specimen. Therefore, this SHT condition was chosen for the C.T.

B. Young’s Modulus of ADC12

Figure 8 presents the measured Young’s modulus of the alloy. Using the measurements, stress–inelastic

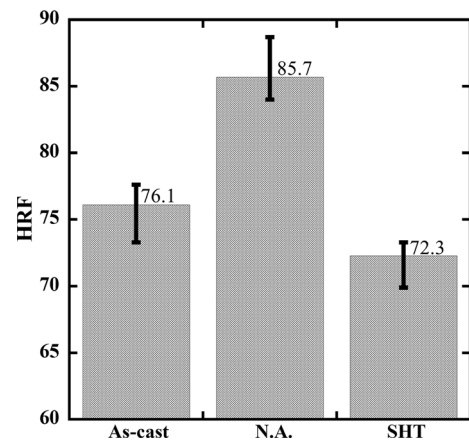


Fig. 6—Change of hardness of ADC12 casting from As-cast condition to natural aging condition (N.A.) and then to solution heat treatment (SHT) after N.A. conditions.

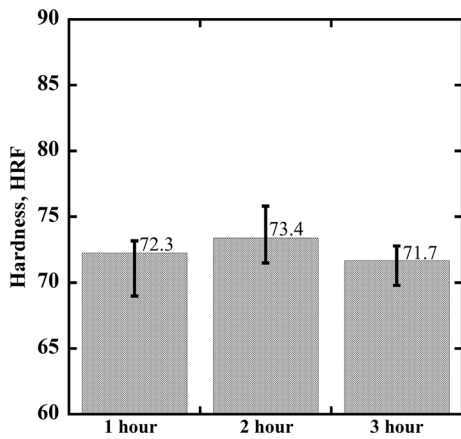


Fig. 7—Effect of solid solution heat treatment time after N.A. condition on ADC12 hardness.

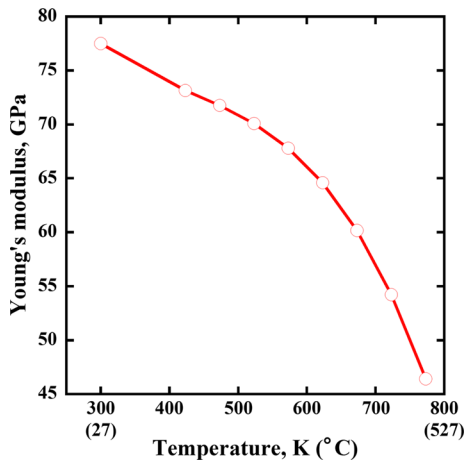


Fig. 8—Young's modulus of ADC12 measured using resonance method.

strain curves were obtained by subtracting the elastic strain component from the true stress–true strain curves at each temperature.

C. Tensile Test

1. Effects of N.A. on stress–strain curves

Figure 9 presents a comparison of stress–strain curves from RT–523 K (250 °C) between the H.T. and C.T. The 0.002 offset yield stresses obtained using the H.T. are approximately 50 to 64 pct higher than those of the C.T. at each temperature. This result indicates that using the stress–strain curves obtained *via* the conventional H.T. method will result in overestimation of the residual stress in the precipitation-strengthening-type aluminum castings.

2. Stress–strain curves obtained using the cooling-test method

Figures 10 and 11 respectively portray the true stress–true strain curves of the alloy obtained by C.T. at 0.001 and 0.0001/s. At temperatures higher than 573 K (300 °C), the stress–strain curves show strong

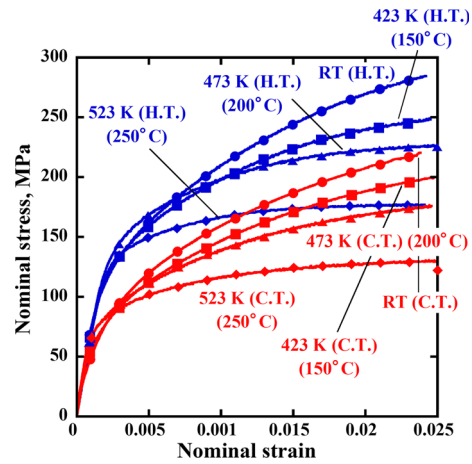


Fig. 9—Comparison of stress–strain curves of ADC12 between heating and cooling tests from RT to 523 K (250 °C).

strain-rate dependence and steady-state flow stresses. Therefore, in this study, temperatures higher than 573 K (300 °C) were designated as the high temperature range, as defined in Section III–A). At temperatures less than 573 K (300 °C), the stress–strain curves start to exhibit strain hardening behavior and less strain-rate dependence with decreasing temperature. Moreover, steady-state flow stress is no longer observed in this temperature range. Therefore, the value of the Norton law “*A*” was changed to approximately 0 from 573 K to 523 K (250 °C to 300 °C) to represent the stress–inelastic curve using, almost exclusively, the plastic terms at temperatures below 523 K (250 °C).

3. Parameters of the constitutive equation

Stress–inelastic strain curves of temperatures higher than 573 K (300 °C) were divided into the initial strain hardening region and the following steady stress region for ADC 12, as shown in Figure 5. The initial strain hardening region was represented by the plastic term. Figure 12(b) shows that the lines of stress–plastic strain relations measured at 0.001/s were inputted in the plastic term. In the Abaqus specification, the plastic term behaves as perfect plasticity (broken lines in Figure 12(b)) when the developed stress reaches the input maximum stress. This stress engenders the unrealistic accumulation of the plastic strain at a high temperature range. To avoid this technical inconvenience, the maximum stresses of the lines at each temperature were selected to be above the steady stresses at the fastest strain rate 0.001/s to prevent the plastic term from activation before activation of the creep term. For creep parameters, the Log steady-state flow stress–Log strain rate graph was made at each temperature. *A* and *n*-values were determined respectively from the constant of proportionality and the intercept in these graphs. Figure 13 presents the determined parameters of the Norton law from 573 K to 723 K (300 °C to 450 °C).

Under 523 K (250 °C) (Figure 12(a)), the obtained true stress–plastic strain curves of 0.001/s were used as input data for the true stress–plastic strain relation in the plastic term at each temperature. However, in Figures 10 and 11,

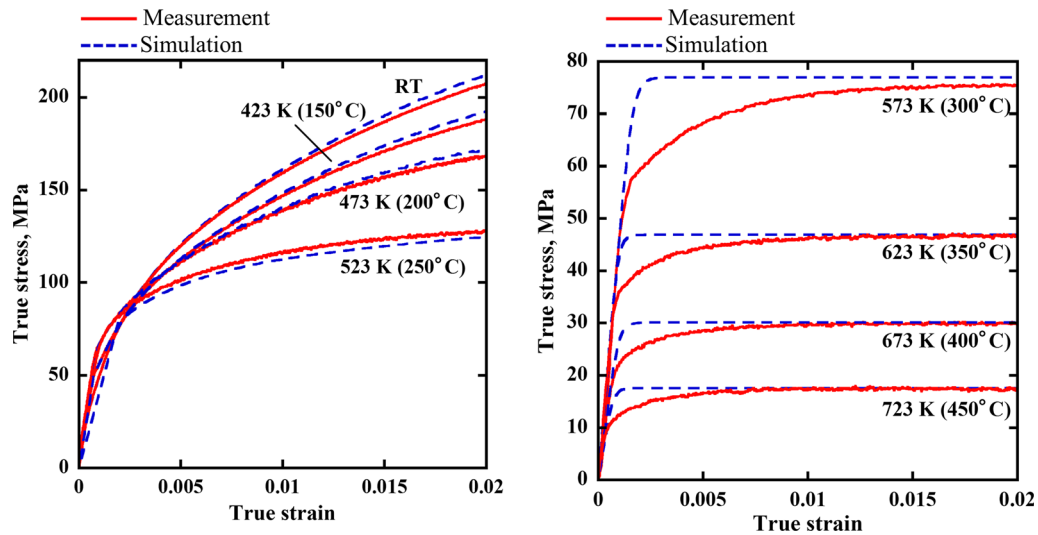


Fig. 10—Comparison of measured and predicted stress–strain response of ADC12 at a 0.001/s strain rate.

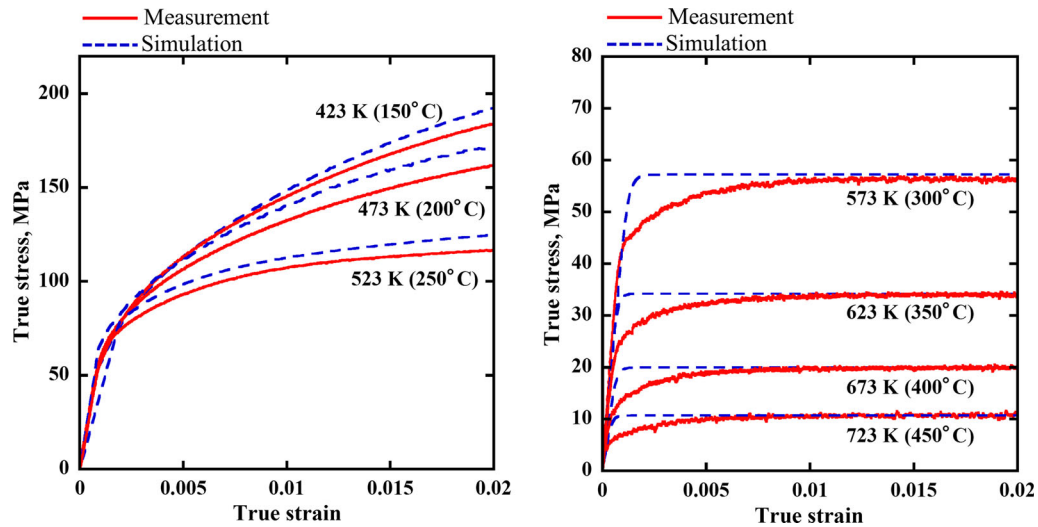


Fig. 11—Comparison of measured and predicted stress–strain response of ADC12 at a 0.0001/s strain rate.

the stress–plastic strain curves measured at 523 K (250 °C) exhibit both strong strain-rate dependence and strain-hardening behavior. Therefore, only at 523 K (250 °C) the stress–inelastic strain curves were obtained at 0.001 and 0.0001/s averaged. This averaged curve was adopted as the stress–plastic strain relation, as described in Section III–B). In the creep term, the “ A ” value in the Norton law was set as $10^{-17.6}$ to 10^{-23} (minimum value of A in the Abaqus) from 573 K to 523 K (300 °C to 250 °C) to prevent development of creep strain below 523 K (250 °C).

V. EVALUATION OF THE DEVELOPED CONSTITUTIVE EQUATION

A. Reproducibility of the Stress–Strain Curves

Figures 10 and 11 respectively present comparisons between the measured and simulated stress–strain curves

at 0.001 and 0.0001/s from RT to 723 K (450 °C). The strain-rate dependence of the stress–strain curves was approximated at temperatures higher than 573 K (300 °C) in the developed constitutive equation. However, the initial strain hardening transient was too extensive at the high temperature range while exhibiting good agreement in the steady-state flow stress region between the simulation and experiment. This excess initial strain hardening estimation is attributable to the usage of the steady-state creep law and to ignorance of the primary creep behavior. Under 523 K (250 °C), the simulated strain hardening behavior of the stress–strain curves was well approximated against the measurement. The slight strain dependence of the stress–strain curves was not duplicated at temperatures lower than 523 K (250 °C) because the creep term almost ceases to function in the developed elasto-plastic-creep constitutive equation at temperatures less than 523 K (250 °C). Therefore, agreement of the stress–strain curves between

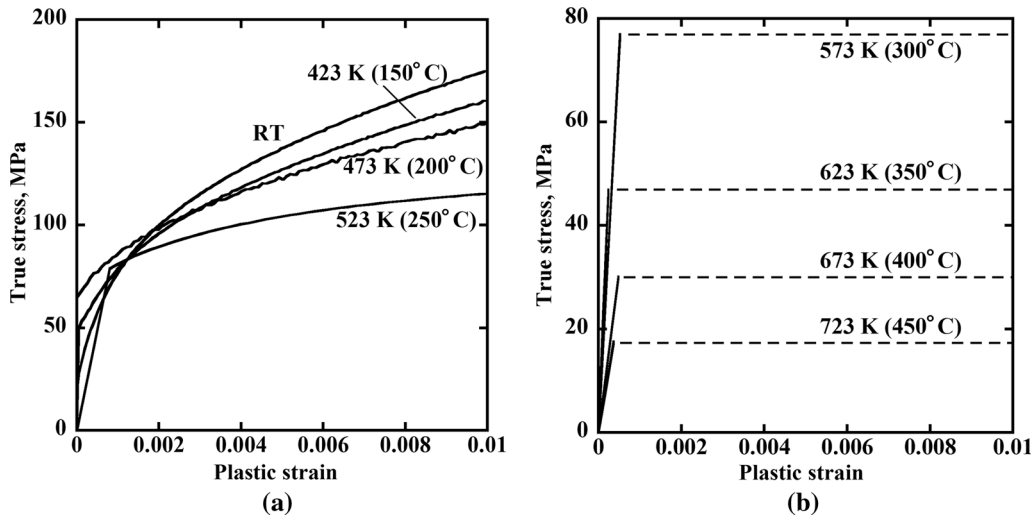


Fig. 12—Inputted true stress–plastic strain curves of ADC12 for Abaqus (a) RT–523 K (RT–250 °C) and (b) 573 K to 723 K (300 °C to 450 °C).

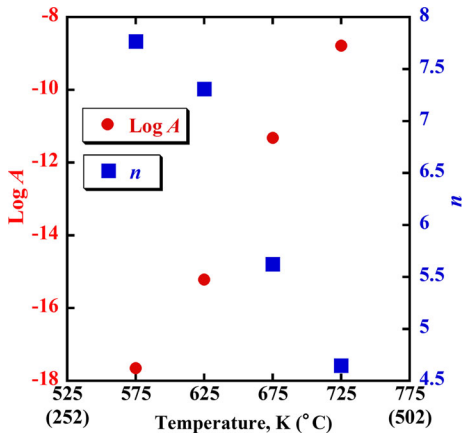


Fig. 13—Inputted creep parameters of ADC12 for Norton law.

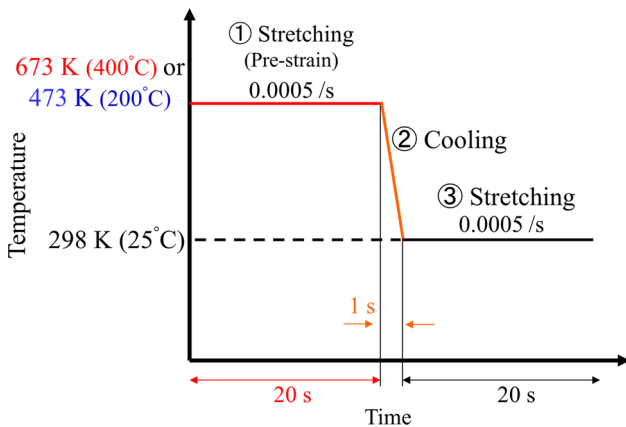


Fig. 14—Temperature and strain history of the specimen in the numerical tensile test.

the simulation and measurements was worse at 0.0001/s than at 0.001/s because the input stress–strain curves were those obtained at 0.001/s.

B. Recovery Behavior of the Developed Constitutive Equation

1. Strain hardening behavior after pre-strain in the high or low temperature range

Figure 14 portrays the temperature and strain history of numerical tensile tests. First, the simple cubic model was stretched, respectively, at 0.0005/s for 20 seconds at 673 K or 473 K (400 °C or 200 °C). 673 K (400 °C) is included in the high temperature range in the developed constitutive equation. 473 K (200 °C) is included in the low temperature range. After cooling to RT [298 K (25 °C)], the calculated model was stretched to 0.01 tensile total strain to elucidate the effects of the developed strain at 673 K or 473 K (400 °C or 200 °C) on strain hardening at RT.

Figure 15 presents the pre-strain effects at each temperature on the strain hardening behavior at RT. The pre-strain at 473 K (200 °C) increases the initial yield stress at the RT, as intended. The pre-strain at 673 K (400 °C) had much less of an effect on strain hardening at RT than that of the 473 K (200 °C). These results demonstrate that almost no inelastic strain developed at the steady-state stress region at 673 K (400 °C) contributed to strain hardening at RT in the developed constitutive equation: this constitutive equation can describe the recovery behavior.

2. Ratios of elastic, plastic, and creep strain in developed total strain at respective temperatures

For further investigation of the recovery behavior at each temperature, the 0.02 tensile total strain was given at each temperature. The respective compositions of the elastic, plastic, and creep strain were obtained. Compositions of the elastic, plastic, and creep strain are portrayed in Figure 16. Results show that almost the entire amount of the given strain became creep strain at temperatures higher than 573 K (300 °C), which was defined as the high temperature range in this constitutive equation for the alloy. Slight plastic strain also occurred

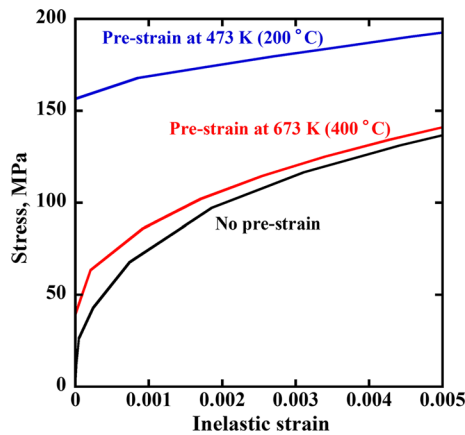


Fig. 15—Effects of pre-strain at 473 K and 673 K (200 °C and 400 °C) on strain hardening behavior at RT, respectively.

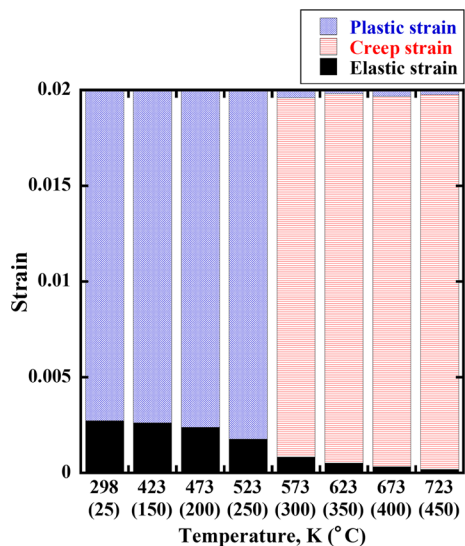


Fig. 16—Ratios of elastic, plastic, and creep strain to 0.02 total strain at respective temperature.

at temperatures higher than 573 K (300 °C). This plastic strain resulted from the initial strain hardening part of the stress–inelastic strain curves at high temperature ranges. Thereby, the developed constitutive equation is useful to prevent plastic strain developed at the high temperature range from accumulating and from contributing strain hardening at the low temperature. Figures 15 and 16 show that our model works well according to the assumption that the inelastic strain developed at the steady-state stress at the high temperature range (above 573 K (300 °C) for this alloy) did not affect the strain hardening behavior of RT. Some earlier studies^[11,17] have demonstrated that aluminum alloy recovery became clearer at temperatures above approximately 573 K (300 °C). Therefore, the recovery behavior of the aluminum alloy can be approximately duplicated by using our equation. Below 523 K (250 °C), plastic strain develops instead of creep strain. This fact demonstrates that all the inelastic strain

developed at temperatures lower than 523 K (250 °C) contributes to strain hardening in the equation.

As demonstrated by the results presented above, this study showed that both the recovery and the strain-rate dependence of the stress–strain curve can be approximated by the model connecting the well-known linear elastic, isotropic hardening plastic, and steady-state creep terms in series. Using the developed constitutive equation, thermal stress analyses of the casting process can be conducted more accurately and more easily than when using the conventional constitutive equation applied in earlier studies.

VI. CONCLUSION

A. Mechanical Properties for the Constitutive Equation of ADC12 (A383.0)

The alloy exhibits N.A. behavior. The Rockwell F scale of the N.A. specimen was about 13 pct higher than that immediately after casting in the alloy. The difference of the hardness was reduced to a 5 pct difference by application of the SHT at 723 K (450 °C) for 1 hour to the N.A. specimen. In tensile tests, the yield stresses of the conventional heating method were 50 to 64 pct higher than those in the tensile test immediately after the SHT. These results demonstrate that using the stress–strain curves measured from the N.A. specimen will cause overestimation of the predicted thermal stress in the castings. The SHT should be applied, followed by cooling to tensile testing temperatures, to obtain stress–strain curves that more closely resemble those during or immediately after casting. These curves should be used for thermal stress analyses of the casting process of the alloy.

B. Constitutive Equation for the Thermal Stress Analysis of the Casting Process

The previous constitutive equation had many material constants or was not based reasonably on the physical basis for describing the recovery and strain-rate dependence of the stress–strain curves. This study suggested the empirical elasto-plastic-creep equation useful for description of these phenomena. In the evaluation of this equation developed for the alloy, the strain-rate dependence at temperatures higher than 573 K (300 °C) was duplicated while preventing almost all the inelastic strain developed above that temperature from contributing to the strain hardening at RT, i.e., strain hardening recovery. Using this model, more accurate prediction of thermal stress analysis can be achieved for aluminum high-pressure die castings.

REFERENCES

1. A.G. Delgado, K.K. Bamoradian, and R.A. Miller: *Die Cast. Eng.*, 2008, vol. 52, pp. 40–46.

2. M.M. Makhlof, D. Apelian, and L. Wang: *North American Die Casting Association Rosemonet*, 1998, IL, pp. 9-16.
3. S. Dong, Y. Iwata, Y. Sugiyama, and H. Iwahori: *Mater. Trans.*, 2010, vol. 51, pp. 371-76.
4. B. Magnin, L. Maenner, L. Katgerman, and S. Engler: *Mater. Sci. Forum*, 1996, vols. 217-222, pp. 1209-15.
5. A.K. Miller: Ph.D. Dissertation, 1975, Stanford University.
6. E. Gustafsson, M. Hofwing, and N. Strömberg: *J. Mater. Process. Technol.*, 2009, vol. 209, pp. 4320-28.
7. P. Hofer, E. Kaschnitz, and P. Schumacher: *JOM*, 2014, vol. 66, pp. 1638-46.
8. Y. Motoyama, H. Takahashi, T. Okane, Y. Fukuda, and M. Yoshida: *Metall. Mater. Trans. A*, 2013, vol. 44A, pp. 3261-70.
9. Y. Motoyama, D. Inukai, T. Okane, and M. Yoshida: *Metall. Mater. Trans. A*, 2014, vol. 45, pp. 2315-25.
10. J. Thorborg, J. Klinkhammer, and M. Heitzer: *Mater. Sci. Eng.*, 2012, vol. 33, p. 012050.
11. H.G. Ejær and A. Mo: *Metall. Mater. Trans. B*, 1990, vol. 21, pp. 1049-61.
12. J.-M. Drezet, O. Ludwig, C. Jacquerod, and E. Waz: *Int. J. Cast Met. Res.*, 2007, vol. 20, pp. 163-70.
13. A. Alankar and M.A. Wells: *Mater. Sci. Eng. A*, 2010, vol. 527, pp. 7812-20.
14. W.M. van Haaften, B. Magnin, W.H. Kool, and L. Katgerman: *Metall. Mater. Trans. A*, 2002, vol. 33A, pp. 1971-80.
15. H. Shiga, T. Sato, H. Kambe, Y. Motoyama, and M. Yoshida: Japan Patent Kokai 2015-132564 (20015.07.23).
16. M. Reich and O. Kessler: *J. Phys.: Conf. Ser.*, 2010, vol. 240, p. 1.
17. N. Chobaut, D. Carron, S. Arsène, P. Schloth, and J.-M. Drezet: *J. Mater. Process. Technol.*, 2015, vol. 222, pp. 373-80.